A comparison of supervised pixel-based color image segmentation methods. Application in cancerology

C Meurie, G Lebrun, O Lezoray, A Elmoataz

A comparison of supervised pixel-based color image segmentation methods. Application in cancerology

C. MEURIE, G. LEBRUN, O. LEZORAY, A. ELMOATAZ
LUSAC EA 2607
University of Caen
BP 78, Site Universitaire, 50130 Cherbourg-Octeville
FRANCE
{cyril.meurie, gilles.lebrun}@chbg.unicaen.fr

Abstract: - In this paper, we describe a new scheme to color image segmentation which is based on supervised pixel classification methods. Using color pixel classification alone does not extract accurately enough color regions, so we suggest to use a strategy based on four steps in different color spaces: simplification, pixel classification, marker extraction and color watershed growing. The strategy is performed on cytological color images. Quantitative measures are used to evaluate the resulting classifications and segmentations with or without a set of reference images.

Key-Words: - Segmentation, pixel classification, color image, quality evaluation

1 Introduction

Images analysis in the field of lung cancer is a diagnosis tool for the cytopathology . The quantitative analysis of the form and the structure of nuclei resulting from microscopic color images brings to the pathologist invaluable information for the diagnosis assistance. This analysis can only be performed from perfectly segmented objects. The segmentation of the bronchial cells is a difficult task because the mucus present in the background has the same aspect as some cells (cytoplasm, nucleus) in the setting of the international coloration of Papanicolaou.

A recent survey [7] showed that an unsupervised pixel classification brought satisfactory results but that a supervised pixel classification could improve our segmentation. That is why, our strategy will be based on this last classification. Therefore, we propose an automatic segmentation scheme based on: a simplification step to reduce the noise, a supervised pixel classification in different color spaces, a marker extraction by using an operation of mathematical morphology and a color watershed growing to segment correctly the objects. The paper is organized as follows : In section 2, we will describe the color segmentation scheme. In section 3, we give experimental results with two evaluation methods. Finally we draw a conclusion.

2 The segmentation scheme

The segmentation scheme (Fig. 1) is given in five steps:

- Image simplification: The simplification step consists in a pre-treatment phase with the aim of smoothing the initial image to reduce the importance of noise. The produced image is used to calculate the gradient needed in the color watershed step. The growing quality depends greatly on the gradient image. This smoothed image is also used as input to the pixel classification step in order to verify the classifier sensitivity to the presence of noise.

Figure 1: The segmentation scheme

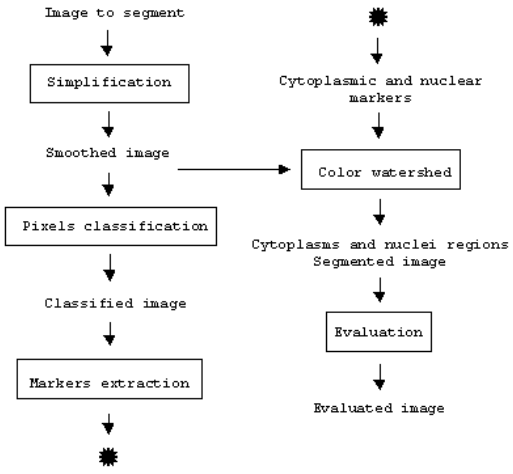

- Pixel classification: The step of classification consists in determining for each pixel of the image, a class among background, cytoplasm or nucleus. To realize this classification, we test several decision functions which have been created by one of the following classifiers: Bayes, kNN, SVM. Each decision function is determined from four images and their expertise in order to create a training base.

- Markers extraction: With the image produced in the previous step, a pixel subset is recognized as belonging to the cytoplasm or the nucleus, this subset corresponds to true markers. The marker extraction is based on mathematical morphology operations which consists in a variable number of erosions according to the marker type.

- color watershed: From the markers previously extracted and the smoothed image, the watershed performs a growing using image color information.

The obtained regions correspond to the cytoplasm and nucleus.

- Evaluation: The evaluation step is composed of two methods corresponding to an evaluation with or without ground truth reference image[1]. The first method is based on an improved classification rate which is adapted to our study. This method gives us a true and false classification rate of the object type. The second method proposed by Liu and improved by Borsotti, is not requiring a ground truth reference image, and allows to compare several segmentations between them.

2.1 Image simplification

The first step of the segmentation is the simplification of a color image I_0 which as increase the global contrast and reduce the noise. The smoothed image I is used as input to the classifiers and as input to a color watershed. To simplify this image, we used a vector image restoration based on the Partial Differential Equations (PDE) which is composed of a diffusion term, a data attachment term and a shock filter term. This function is defined by [13]:

$$\begin{aligned}\frac{\partial I}{\partial t} = g_r(\sqrt{\lambda_+})I_{\eta\eta} + I_{\xi\xi} + \\ \alpha_a(I - I_0) - \\ \alpha_c(1 - g_r(\sqrt{\lambda_+}))U\end{aligned} \quad (1)$$

where

$$U = \begin{pmatrix} sign(I^1_{\eta\eta})||(I^1_\eta)|| \\ sign(I^2_{\eta\eta})||(I^2_\eta)|| \\ \dots \\ sign(I^n_{\eta\eta})||(I^n_\eta)|| \end{pmatrix} \quad (2)$$

The free parameters α_a and α_c weight the importance of the shock filter and of the data attachment in the diffusion process. They are fixed by hand. $\sqrt{\lambda_+}$ denotes the color gradient norm, η and ξ are its corresponding direction and $g_r(.)$ is a decreasing function.

$$g_r(s) = exp(-\frac{s^2}{2r^2}) \quad (3)$$

2.2 Pixel classification

2.2.1 Training bases

Our pixel classification belongs to supervised classifiers techniques. For it, we generate a training base from four images containing objects with a wide variability. These images have been manually segmented by an expert in cytopathology (Fig. 2). A testing base was also created from four other representative images.
With Bayes classifier, a training base is generated with all the pixels of the images. With kNN and SVM classifiers, an evaluation has showed that the training time on all pixels of the images is too important. An alternative consists in learning on a pixel subset. This subset is built by selecting randomly n pixels from the three classes: background, cytoplasm, nucleus in each images. This method guarantees that every classes is sufficiently represented.

Figure 2: An initial image (a: left) and the reference image (b: right)

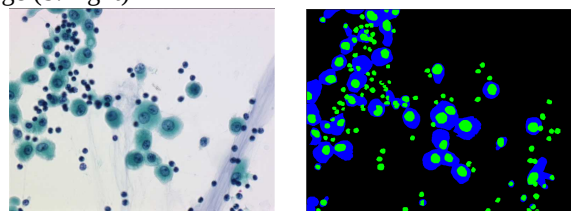

2.2.2 Classification methods

In this section, we present the three classifiers which are used : Bayes, kNN, SVM (Fig. 3).

- Bayes: This classifier is based on the Bayesian decision theory. It is a supervised statistical approach to pattern classification which assumes that the decision problem is expressed in probabilistic terms. Since the algorithm is dealing with color images, a mixture of Gaussian distribution models is used. For each element x, the class that maximizes the probability to contain this element is searched.

$$\begin{aligned}f(x,i) = -\frac{1}{2}(x-\mu_i)^T \Sigma_i^{-1}(x-\mu_i) \\ -\frac{1}{2}\log|\Sigma_i| - \log p_i + \frac{n}{2}\log 2\pi\end{aligned} \quad (4)$$

  where n is the number of classes , μ_i the mean attribute vector, Σ_i is the conditional covariance matrix and p_i the prior probability of class i.

- kNN: The k Nearest Neighbors method is well known used for many years in the field of machine learning [9]. Given a training set and a distance defined in the attribute space, the basic kNN rule consists in searching for the k nearest neighbors of an attribute vector. The estimated class probabilities is proportional to the number of C_j class among k nearest neighbors (with $1 \leq j \leq n$ and n is the number of classes in the training set), then the chosen j corresponds to the class which has the maximum probability. The value of k must be chosen to minimize the expectation of test error.

- SVM: The Support Vector Machine method has received a considerable attention in the recent years and many successful applications of SVM have been described in the literature [2, 14]. The objective of SVM is to maximize the margin of separation

[1]The authors would like to thank Mr M. Lecluse and the pathological anatomy and cytology department of the Louis Pasteur Hospital Center of Cherbourg for providing the ground truth reference images

between the classes. Larger margin ensures smaller Vapnik and Chervonenkis (VC) dimension, which yields a good generalization performance. SVM are learning systems that use hypothesis space of linear functions by projecting the data into a high dimensional feature space. The use of kernel function $k(.,.)$ (example: a Gaussian kernel) implicitly performs a non-linear mapping to a high dimension feature space reducing the training of a SVM to maximizing a convex quadratic form subject to linear constraints. The maximum margin hyperplane found with SVM can be represented as a linear combination of training points called support vectors. Many specific algorithms can solve the convex quadratic problem of SVM, the most competitive being Sequential Minimal Optimization [10]. It remains two hyper-parameters (C and σ) that must be chosen to minimize the expectation of test error. The training algorithm produce a decision function where each support vectors has a α_i value characterizing his weight on the hyperplane position. For multiclass problem many binary SVMs are trained and the one which have maximal output defines the class of example.

$$k(x_i, x_j) = \exp\left(\frac{-\parallel x_i - x_j \parallel^2}{2\sigma^2}\right) \quad (5)$$

$$\varphi(x) = \sum_{i \in SV} \alpha_i y_i k(x_i, x) + b \quad (6)$$

where $0 \leq \alpha_i \leq C$ and (x_i, y_i) is an example of the training base.

Figure 3: The classified images

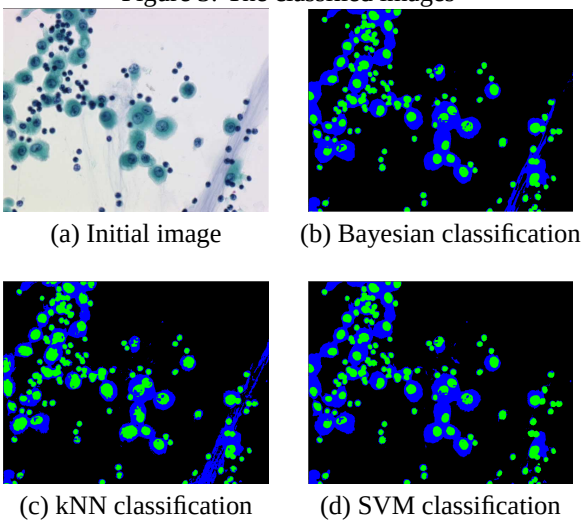

(a) Initial image (b) Bayesian classification

(c) kNN classification (d) SVM classification

2.3 Color watershed

Using the markers obtained at the preceding stage, we seek to locate precisely the contours of the regions (Fig. 4). For that, we use a color watershed [15, 8, 12] which aim to carry out a growing. This growing uses previously extracted seeds to propagate the labels in the image according to an aggregation function. The color watershed used in this paper is defined according to a specific aggregation function. This function defines the aggregating probability of a pixel to a region. It is based on two main information describing the spatial information of the image: local information expressed by the color gradient processed with the DiZenzo's definition [3]) and global information expressed with the Euclidean distance by the color mean of the regions describing their color homogeneity. The aggregation function is defined by [4, 5]:

$$f(p, R) = (1 - \alpha)\|I(R) - I(p)\| + \alpha\|\nabla I(p)\| \quad (7)$$

where $I(R)$ the mean color vector of the region R for the image I, $I(p)$ the vector giving the color of a pixel P and $\nabla I(p)$ the color gradient. α is a blending coefficient [5] which allows to modify the influence of the local criteria compared to the global criteria during the growing process (see in [5] for more details).

Figure 4: The segmented images

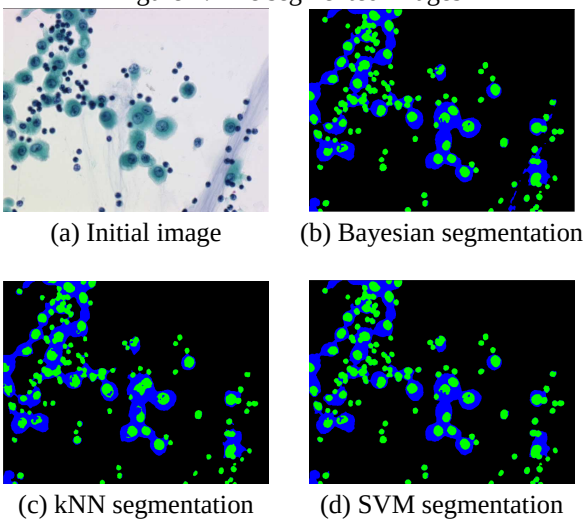

(a) Initial image (b) Bayesian segmentation

(c) kNN segmentation (d) SVM segmentation

3 Experimental results

3.1 Evaluation methods

Our study on the abnormal cells detection should allow to improve the quality of the diagnosis. The resulting evaluation step is then very important. We compare results at the output of the pixel classification step (classified image) and at the end of treatment (segmented image) in order to choose the best classifier and evaluate the color watershed importance. For that, two methods are used: one has been proposed by Liu [6] and has been improved by Borsotti [1]. The second, our method is based on a classification rate which is adapted to our study.

3.1.1 Evaluation of Liu

Liu's evaluation: This method provides a quality estimation which enables to compare several segmentations between them. Moreover, it doesn't need to have ground truth reference image.

$$Q(I_M) = \frac{1}{1000NM}\sqrt{R}\sum_{i=1}^{R}\frac{e_i^2}{1+log(A_i)} \quad (8)$$

with I_M is the segmented image, $N.M$ the size of this image, R the number of regions in the segmented image, A_i the number of pixels of the ith region, e_i the color error of region i. The color error is calculated as the sum of the Euclidean distances between the color components of the pixels and the average of their regions. More Q is low, better is the segmentation. But this method requires some precautions: regions must be uniform and homogeneous. The inside of regions must be simple without too many holes, and the adjacent regions must have significant differences in colors.

3.1.2 Our evaluation method

Our method is an extension method based on a rate of classification [11]. This method uses a reference segmentation in order to provide true or false classification rate on the cytoplasm and the nucleus. The image that we analyze presents a variable number of cells. To compute these rates, we calculate the number of pixels belonging to every classes in the image. The common rate (ComCyt or ComNuc) shows the number of pixels which are correctly identified in the reference image. Whereas the difference rate (DifCyt or DifNuc) globalizes for a C class (cytoplasm or nucleus), the two following errors: a pixel of the C class in the reference image is not recognized as the same class in the segmented image, and a pixel not being of the C class in the segmented image is recognized as the C class in the reference image. We use the $delta$ term to globally evaluate the classification and segmentation rate based on the $AvCom$ and $AvDif$ terms. $AvCom$ is a weighted average from $ComCyt$ and $ComNuc$ in according to the pixel number of each class. $AvDif$ is calculate in the same way.

$$ComCyt = \frac{\left|E^R_{\{C\}} \cap E^A_{\{C\}}\right|}{\left|E^R_{\{C\}}\right|} \quad (9)$$

$$ComNuc = \frac{\left|E^R_{\{N\}} \cap E^A_{\{N\}}\right|}{\left|E^R_{\{N\}}\right|} \quad (10)$$

$$DifCyt = \frac{\left|(E^R_{\{C\}} \cap E^A_{\{B\}}) \cup (E^R_{\{B\}} \cap E^A_{\{C\}})\right|}{\left|E^R_{\{C\}} \cup E^A_{\{C\}}\right|} \quad (11)$$

$$DifNuc = \frac{\left|(E^R_{\{N\}} \cap E^A_{\{B,C\}}) \cup (E^R_{\{B,C\}} \cap E^A_{\{N\}})\right|}{\left|E^R_{\{N\}} \cup E^A_{\{N\}}\right|} \quad (12)$$

$$Delta = AvCom - AvDif \quad (13)$$

$$E^{\beta}_{\alpha} = \{(x,y) \in I : I_{\beta}(x,y) \in \alpha\}$$

with B : background, C : cytoplasm, N : nucleus, R : reference image, A : automatic image

Figure 5: Segmentation results with Liu's evaluation in different color space

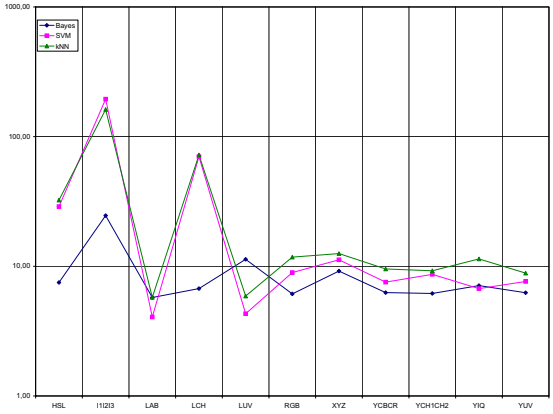

Figure 6: Segmentation results with our evaluation in different color space

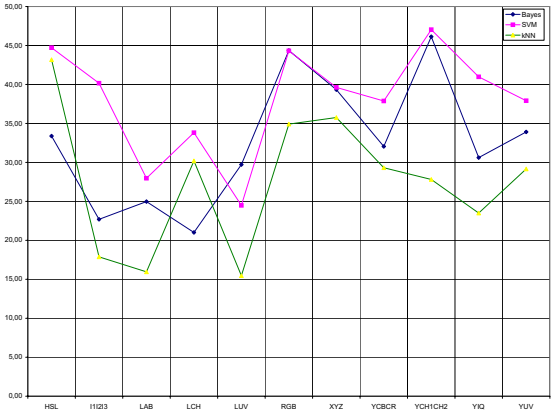

3.2 Evaluation of the proposed scheme

The images come from microscopic cytology images of bronchial tumours. We present the classification and segmentation results obtained on 4 cytologycal color images 24 bits of 574*752 pixels, each one containing about one hundred cells. For readability reasons, we present only the results of each classifier with his best parameters and in the different color spaces among: RGB, XYZ, LUV, LAB, LCH, YIQ, YUV, YC_bC_r, YCh_1Ch_2, $I_1I_2I_3$, HSL (Tables 1, 2, 3, 4 and Fig. 6, 5).

In the table 1, the columns C1 and S1 correspond to a base constructed with n=334 and C2 and S2 with n=1002. C corresponds to results of the pixel classification and segmentation with SVM. We show that the segmentation step improves the recognition of nuclei but decreases the recognition of cytoplasms. Globally the gap (AvDif) is increased and therefore the segmentation is improved. Moreover, we show that the increase in size of the training base increases the treatment time but doesn't improve the segmentation rate. We also have noted this phenomenon with kNN. Thereafter, we will only use the results obtained with n=334.

Table 1: Improvement due to the segmentation step with SVM (n_{C1}=334 et n_{C2}=1002)

	C1	S1	C2	S2
ComCyt	77.6 %	64.1 %	75.9 %	62.6 %
ComNuc	85 %	91.1 %	87 %	92.2 %
AvCom	80.7 %	74.5 %	80.4 %	73.9 %
DifCyt	36.6 %	41.1 %	32.9 %	39.4 %
DifNuc	37.4 %	37.5 %	38.3 %	38.2 %
AvDif	38.5 %	42.3 %	37.3 %	41.9 %
Delta	**42.2**	**32.2**	**43.1**	**32**

In the table 2, the column S1 corresponds to the segmentation gotten from a smoothed image base, and S2 from a initial image base. The improvement of the S2 segmentation is low compared to the S1 segmentation, but as this smoothed image is necessary to the color watershed, all following training will be achieved from the smoothed image.
We present segmentation results for every classifiers, in order to show the noise importance of the color space (Fig. 6, 5). For our evaluation method, we keep the three best color spaces. For Bayes, the best color spaces are YCh_1Ch_2, RGB, XYZ. For SVM, the best are: YCh_1Ch_2, HSL, RGB. For kNN, the best are HSL, XYZ, RGB. Color spaces providing the best Liu's estimation have not been taken in account in this ordering.

Table 2: Results with (S2) and without (S1) simplification step with kNN

	S1	S2
ComCyt	64.6 %	68.2 %
ComNuc	80.6 %	82.7 %
AvCom	71.6 %	74.4 %
DifCyt	22.3 %	23.4 %
DifNuc	40.6 %	37.2 %
AvDif	32.9 %	31.2 %
Delta	**38.7**	**43.2**
Liu	65.7	32.4

The table 3 and 4 deals with the best classification and segmentation results obtained with the three classifiers. We indicate for every classifier, the space on which we obtained the best results. The SVM gives better results in segmentation than Bayes but their computational times are longer important (with a PC 2Ghz - 512Mo RAM: Bayes= 2s, kNN= 420s, SVM= 120s).

Table 3: The best classifications with different classifiers

	Bayes	SVM	kNN
Space	YCh_1Ch_2	YCh_1Ch_2	HSL
ComCyt	78.9 %	79.3 %	83.6 %
ComNuc	83.8 %	83.7 %	78.8 %
AvCom	80.6 %	81.2 %	82.7 %
DifCyt	34.1 %	24.6 %	23.7 %
DifNuc	34.6 %	35.4 %	38.7 %
AvDif	34.8 %	30.1 %	31.8 %
Delta	**45.7**	**51**	**50.9**

Table 4: The best segmentations with different classifiers

	Bayes	SVM	kNN
Space	YCh_1Ch_2	YCh_1Ch_2	HSL
ComCyt	70.2 %	70.9 %	68.2 %
ComNuc	88.2 %	87.4 %	82.7 %
AvCom	77.1 %	77.4 %	74.4 %
DifCyt	27.9 %	24.5 %	23.4 %
DifNuc	34.9 %	35 %	37.2 %
AvDif	31 %	30.4 %	31.2 %
Delta	**46.1**	**47**	**43.2**
Liu	6.2	8.7	32.4

4 Conclusion

We proposed a segmentation color scheme to cytological images. We show the importance of each steps (simplification, pixel classification, marker extraction, color watershed growing). The study shows the importance of the choice of supervised classifiers and of the color spaces. Our method is adapted to the segmentation of color objects in a noisy environment (under some restrictions) and particularly to the segmentation of cellular objects. We obtained very good results on the segmentation of nuclei in accordance with our waiting ($>$ 87 %) as well as the segmentation of cytoplasms ($>$ 83 %).
In order to improve the cytoplasm segmentation, we will consider a marker adaptive extraction step depending on the quality of the pixel classification. Another improvement will consist in selecting a smaller subset of the training base which would improve the pixel classification and the computational time.

References:

[1] M. Borsotti, P. Campadelli, and R. Schettini. Quantitative evaluation of color image segmentation results. *Pattern recognition letters*, 19:741–747, 1998.

[2] N. Cristianini and J . Shawe-Taylor. *Introduction to Support Vector Machines and other kernel-based learning methods*. Camridge University Press, 2000.

[3] S. DiZenzo. A note on the gradient of a multi-image. *Computer Vision, Graphics and Image Processing*, 33:116–126, 1986.

[4] O. Lezoray and H. Cardot. Cooperation of color pixel classification schemes and color watershed : a study for microscopical images. In *IEEE transactions on Image Processing*, volume 11-7, pages 783–789, 2002.

[5] O. Lezoray and H. Cardot. Histogram and watershed based segmentation of color images. In *Proceedings of CGIV'2002*, pages 358–362, 2002.

[6] Liu and Y-H. Yang. Multiresolution color image segmentation techniques. *IEEE Transactions and Pattern Analysis and Machine Intelligence*, 16:689–700, 1994.

[7] C. Meurie, O. Lezoray, H. Cardot, and A. Elmoataz. Comparaison de classifieur non-supervisés pour la segmentation d'images couleur. application en imagerie biomédicale. In *International Conference on Image and Signal Processing*, Juin 2003.

[8] F. Meyer. Color image segmentation. In *Proceedings of the International Conference on Image Processing and its Applications*, pages 303–306, 1992.

[9] D. Michie, DJ. Spiegelhalter, and CC. Taylor. Machine learning, neural and statistical classification. volume 6, pages 84–106, 1994.

[10] J. Platt. Sequential minimal optimization: A fast algorithm for training support vector machines. In *Advances in Kernel Methods - Support Vector Learning*, pages 185–208, 1998.

[11] S. Schupp, A. Elmoataz, P. herlin, and D. Bloyet. Mathematical morphologic segmentation dedicated to quantitative immunohistochemistry. In *Anatycal and Quantitative Cytolgy and Histology*, volume 23, 2001.

[12] L. Shafarenko, M. Petrou, and J. Kittler. Automatic watershed segmentation of textured color images. *IEEE transactions on Image Processing*, 6(11):1530–1543, 1997.

[13] D. Tschumperlé and R. Deriche. Constrained and unconstrained pde's for vector image restoration. In *Proceedings of SCIA'2001*, pages 153–160, 2001.

[14] V.N. Vapnik. In *Statistical Learning Theory*. Wiley, 1998.

[15] L. Vincent and P. Soille. Watersheds in digital spaces : An efficient algorithm based on immersions simulations. *IEEE transactions on PAMI*, 13(16):583–598, 1991.